

# Adsorption Profile of N5 Acyclic Ligand Derived from 1, 2-Diamino Benzene and 2, 6-Diacetylpyridine on Column Packed Calcined Iraqi Montmorillonite

Mohammed H. Abdul Latif<sup>1\*</sup>, Taghreed M. Musa<sup>2</sup>, Mohammed A.K. Alsouz<sup>2</sup>

1. Department of Chemistry, Ibn Al Haitham College of Education, University of Baghdad, Adhamiya, Al-Dilal Square, Baghdad, Iraq

2. Chemistry department, College of science, Al-Mustansiriya University, Al-Mustansiriya, Baghdad, Iraq  
Email: mohammed21latif@yahoo.com

## Abstract

The adsorption ability of IRAQI initiated burned granulated bentonite of ligand (L), from aqueous solutions has been investigated through columnar method. The ligand (L) adsorption was found to be dependent on adsorbent dosage, initial concentration and contact time. All columnar experiments were carried out at three different pH values (5.5, 7 and 8) using buffer solutions at flow rate of (3 drops / min.) at room temperature (25±2) °C. The experimental isotherm data were analyzed using Langmuir, Freundlich and Temkin equations. The monolayer adsorption capacity is 0.7055 mg ligand (L) per 1g burned bentonite. The experiments showed that highest removal rate was 88.25% for ligand (L) at pH 7. The kinetic data for the adsorption process obeyed pseudo-second-order rate equations.

**Keywords:** N5 acyclic ligand, Adsorption Profile, Iraqi Montmorillonite, Column Packed.

## 1. Introduction

Schiff bases derived from an amino and carbonyl compound are an important class of ligands that coordinate to metal ions via azomethine nitrogen and have been studied extensively [1]. In azomethine derivatives, the C=N linkage is essential for biological diuretic activities [2]. Schiff bases have wide applications in food industry, dye industry, analytical chemistry, catalysis, Fungicidal; agrochemical and biological activities [3]. With the increasing incidence of deep mycosis there has been increasing emphasis on the screening of new and more effective antimicrobial drugs with low toxicity. Schiff bases derived from 2, 6-diacetylpyridine and 2-pyridine carboxaldehyde with 4-amino-2, 3-dimethyl-1-phenyl-3-pyrazolin-5-one show antibacterial and antifungal activities [4].

Clay minerals are the most important inorganic components in soil due to their excellent adsorption properties [5]. Natural mineral clays possess specific surface chemical properties, e.g., cation exchange capacity, and adsorptive affinity for some organic and inorganic compounds. Bentonite is an absorbent aluminum phyllosilicate, essentially impure clay consist in mostly of montmorillonite. There are different types of bentonite, each named after the respective dominant element, such as potassium (K), sodium (Na), calcium (Ca), and aluminum (Al). Bentonite clay deposits are mostly composed of clay minerals, a subtype of phyllosilicate minerals, which imparts plasticity and harden when fired or dried [6]. Montmorillonite possess adsorption properties mainly because of their colloidal nature which stems from their very small particle size. The structure of montmorillonite is an octahedral alumina sandwiched between two tetrahedral silica sheets to form the structural unit. Variations in interstitial water and exchangeable cations in the interlayer space affect the properties of bentonite [7]. Vermiculite and bentonite are clay minerals with high CEC. The CEC for vermiculite, for instance, is approximately 100– 150 meq. Per 100 g. The surface area for west Iraqi (Traifawi) bentonite was estimated using methylene blue (MB) adsorption method and it was (123 m<sup>2</sup> /g) [8]. West Iraqi (Traifawi) bentonite consists mostly of calcium – montmorillonite. The percent of montmorillonite is between (60 – 65 %) of crude bentonite, (Table 1) show the chemical analysis of West Iraqi (Traifawi) bentonite. Therefore it is necessary to remove the impurities before the bentonite is ready to use [9].

Table 1

West Iraqi (Traifawi) bentonite chemical analysis.

Compound	SiO <sub>2</sub>	Al <sub>2</sub> O <sub>3</sub>	Fe <sub>2</sub> O <sub>3</sub>	CaO	MgO	Na <sub>2</sub> O	K <sub>2</sub> O	LiO <sub>2</sub>	SO <sub>3</sub>	L.I.O.	Total
Weight %	55.81	14.91	5.78	5.72	3.5	1.29	0.41	0.67	---	10.86	99.67

In the present article we investigate the adsorption of a synthesized and characterized penta dentate ligand (L) derived from 2, 6-diacetylpyridine and 1, 2-diamino benzene on the surface of calcined initiated Iraqi Montmorillonite clay packed in glass columns, and calculate the effect of factors like pH, ionic strength contact time and weight of clay on percentage of removal of the ligand (L), also calculate the isothermic factors of adsorption process..

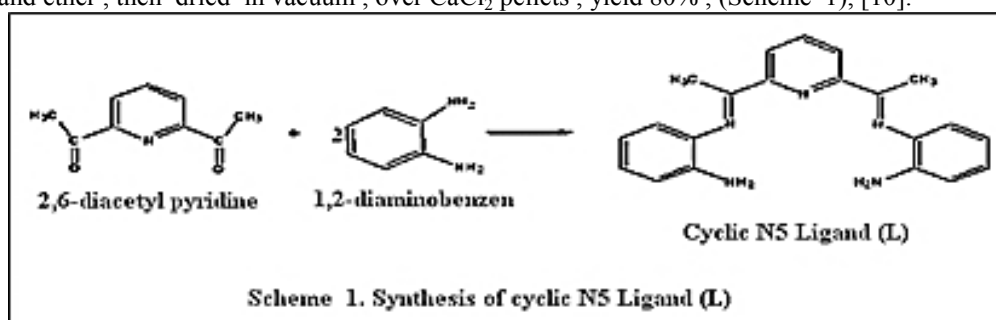
## 2. Materials and methods

### 2.1. Materials

All Chemicals used were of analytical reagent grad unless otherwise is mentioned, Reagents were supplied from Fluka, BDH chemicals. Distilled and deionized water with conductivity value of  $1.5 \times 10^{-5} \text{ S cm}^{-1}$  was used in all experiments. Bentonite mineral clay obtained from the General Company for Geological Survey and Mining in Baghdad, Iraq. The samples were sieved to produce the desired particle size fractions. The samples with a particle size  $45\mu\text{m}$  was then dried for 24 h at  $110^\circ\text{C}$  in an electric oven and stored in a desiccator until use.

### 2.2. Preparation of the ligand N5 (L).

A 20 ml methanolic solution of 2,6-diacetyl pyridine( 0.02 mole ,3.26g), was refluxed with 100cm<sup>3</sup> methanolic solution of recrystallized 1,2-diaminobenzen ( 0.01 mole,1.08 g) for about 4 hrs. A few drops of glacial acetic acid were added to the mixture and refluxed continued for about 12 hrs. The mixture was concentrated to half of its volume and kept in desiccators. The ligand was filtered, washed with methanol , acetone and ether , then dried in vacuum , over  $\text{CaCl}_2$  pellets , yield 80% , (Scheme 1), [10].



### 2.3. Preparation of buffer and stock solutions.

Three phthalate and phosphate buffer solutions of pH values (5.5, 7, and 8) were prepared respectively, also a three stock solutions of the prepared ligand (L) of 2000 mg /L concentration prepared in 100 ml volumetric flask using the above buffer solutions.

### 2.4. Procedure for synthesis of granulated Iraqi Burned Initiated Na – montmorillonite clay.

In this study the bentonite was beneficiated to improve its Smectite (Montmorillonite) content by attrition – scrubbing at high solid concentration (50%) and at high impeller speed (2500 r.p.m.) for 1 h, using flotation cell. In order to convert calcium - montmorillonite to sodium - montmorillonite the process performed by mixing the bentonite pre concentrate with Na – form activated amberlight orange ion exchanger followed by agitation for 1 h, at 150 r.p.m. The clay was separated from the mixture by filtration, washed five times with distilled water. Each washing step involved stirring the slurry in distilled water, followed by centrifugation and removal of the supernatant, the obtained Na – montmorillonite finally treated with 0.5 M NaCl to ensure complete transformation to the Na – form, then the treated clay was washed with distilled water to remove excess NaCl, turned to a granules of (2mm) diameter using granulating machine ( GK Dry Granulating Machine ) and dried at  $110^\circ\text{C}$  for 3h, until constant mass, and then burned at  $650^\circ\text{C}$  to make an ion – exchange column ready to use.

### 2.5. Columnar adsorption procedure.

Three standard solutions of ligand (L) 30 mg /L concentration were prepared from stock solutions of ligand (L) in different pH values (5.5, 7and 8) using buffer solutions. UV-Visible scanning spectrum has been recorded and wavelength value corresponding to the maximum absorption found to be at (423 nm for pH = 5.5), (420 nm for pH = 7), and (424 nm for pH = 8), as shown in (Figure 1), (Figure 2), and (Figure 3) Respectively, these values choose for measurements of estimation throughout this research.

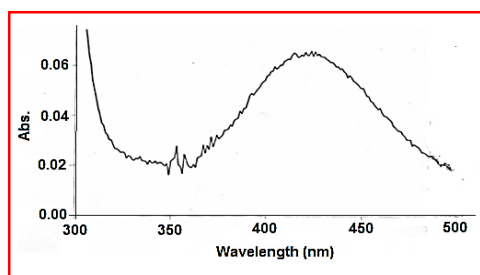


Figure 1. Scanning graph of Ligand L, Buffer soln. pH = 5.5, Conc. = 30 ppm.,  
At  $\lambda_{\text{max.}} = 423 \text{ nm}$ .

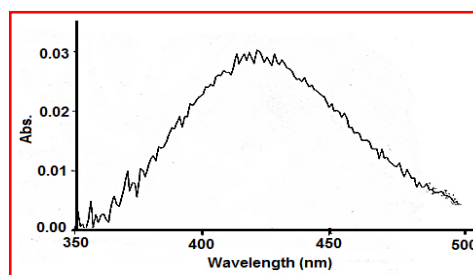


Figure 2. Scanning graph of Ligand L, Buffer soln. pH =7, Conc. = 30 ppm.,  
At  $\lambda_{\text{max.}} = 420 \text{ nm}$ .

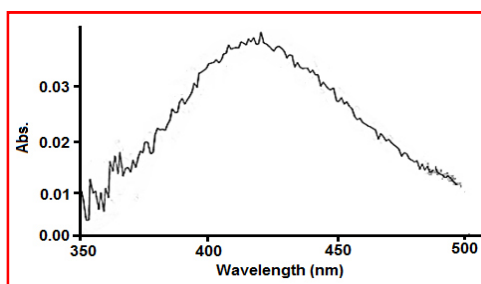


Figure 3. Scanning graph of Ligand L, Buffer soln. pH = 8, Conc. = 30 ppm.  
At  $\lambda$  max. = 424 nm.

Seven standard solutions of ligand (L) in the range of (5 - 35 ppm or mg /L) concentration were prepared from stock solutions of ligand (L) at different pH values (5.5, 7 and 8) using buffer solutions. The absorbance of each solution was measured at  $\lambda$  max. (423 nm for pH = 5.5), (420 nm for pH = 7), and (424 nm for pH = 8) respectively against blank (buffer solution corresponding to pH value). Calibration curves were drawn between absorbance and concentration of ligand (L) standard solutions, as shown in (Figure 4), (Figure 5), and (Figure 6) respectively.

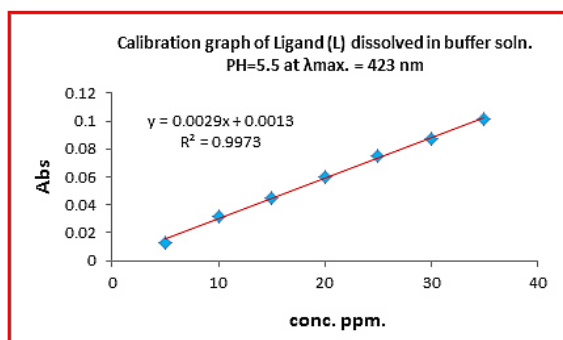


Figure 4. Calibration curve of Ligand L dissolved in buffer soln. pH = 5.5 at  $\lambda$  max. = 423 nm.

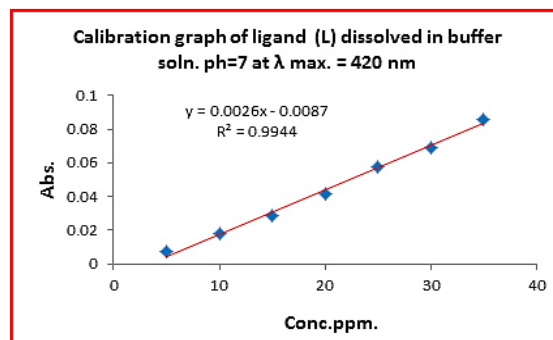


Figure 5. Calibration curve of Ligand L dissolved in buffer soln. pH = 7 at  $\lambda$  max. = 420 nm.

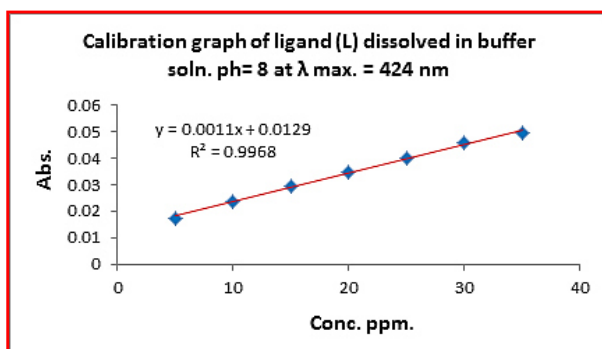


Figure 6. Calibration curve of Ligand L dissolved in buffer soln. pH = 8 at  $\lambda$  max. = 424 nm.

A six glass columns (50 cm X 10 mm i.d.) filled with known mass (1gm) of natural mineral clay adsorption bed (Initiated Burned Na - montmorillonite) corresponding to bed heights of (17mm) (the surface area of 1 gm. mass of natural clay adsorption bed was calculated physically and its found to be 23.904  $\text{cm}^2$ ) have been prepared to run (10 ml) of each of (50 - 100 mg/L) ligand (L) solutions adjusted to different pH values (5.5, 7 and 8) using buffer solutions at flow rate of (3 drops/ min.) at room temperature ( $25 \pm 2$ )  $^\circ\text{C}$ . Then we examine the percolated solutions by measuring the absorbance of each solution at fixed  $\lambda$  max. That have been identified for each pH value, using (UV-Vis - 1800 Shimadzu Spectrophotometer). The equilibrium adsorption uptake and percent removal of ligand (L) from the aqueous solution  $q_e$  (mg/g) was calculated using the relationship noted at the bottom of the (Table 2).

Table 2  
 Adsorption parameters of adsorption of ligand (L) on initiated burned Iraqi bentonite clay mineral.

Sorbent ligand (L) concentration $C_0$	pH 5.5			pH 7			pH 8		
	$C_e$	Removal %	$q_e$	$C_e$	Removal %	$q_e$	$C_e$	Removal %	$q_e$
50	9.85	80.3	0.4015	7.85	84.30	0.4215	9.6	79.50	0.404
60	10.90	81.8	0.4910	8.65	85.50	0.5135	13.7	77.16	0.463
70	11.60	83.4	0.5840	9.40	86.50	0.6060	18.2	74.00	0.518
80	12.65	84.2	0.6735	10.20	87.25	0.6980	22.3	72.12	0.577
90	16.55	82.6	0.7345	10.95	87.83	0.7905	28.0	68.80	0.620
100	18.35	82.6	0.8165	11.75	88.25	0.8825	32.3	67.70	0.677

Amount adsorbed  $q_e = (C_0 - C_e)V/W$  (mg of adsorbate / g of adsorbent), removal % =  $100(C_0 - C_e) / C_0$ , Where  $C_0$  is the initial sorbate concentration (mg/L),  $C_e$  the equilibrium adsorbate concentration (mg/L), V is the volume of solution in L and w is the mass of the adsorbent in (g) [11].

### 3. Results and discussion

#### 3.1. Characterization of bentonite clay mineral.

Natural Iraqi bentonite was characterized by FT-IR spectroscopic analysis (Shimadzu FTIR Spectrometer – 3000:1/ IRAff). FT- IR spectrum (Figure 7. A) showed absorption band at  $3628.10\text{ cm}^{-1}$  (Al-OH) (Mg-OH) corresponding to vibration of structural OH stretching groups coordinating to Al-OH or Mg-OH. Adsorbed water gives a broad bands from  $4306.29\text{ cm}^{-1}$  to  $3533.59\text{ cm}^{-1}$  corresponding to  $\text{H}_2\text{O}$ - stretching vibration. Al, Mg bound water molecules gives H-O-H stretching vibration bond at  $1643\text{ cm}^{-1}$ . Also three bands at  $1546.91$ ,  $1427.32$  and  $1384.89\text{ cm}^{-1}$  corresponding to H...O...H weak. The complex broad band around  $1033\text{ cm}^{-1}$  belongs to Si-O stretching vibration. Two bands at  $914.26\text{ cm}^{-1}$  and  $837.11\text{ cm}^{-1}$  are most characteristic for quartz. Finally the bands from  $420.00\text{ cm}^{-1}$  to  $516.93\text{ cm}^{-1}$  are related to Al-O-Si, Si-O-Si deformations. Initiated bentonite FT-IR spectrum (Figure 7. B) Showed the same bands of (Figure 7. A) but with higher transmittance percent and sharper than bands of FT- IR spectrum of natural bentonite. Nevertheless H...O...H weak disappear in this spectrum. Adsorbed water band appear at  $4321.72\text{ cm}^{-1}$ , two bands belong to Al, and Mg bound water molecules observed at  $1654.92\text{ cm}^{-1}$  and  $1641.42\text{ cm}^{-1}$ . The broad complex band becomes single band at  $1039\text{ cm}^{-1}$  belongs to Si-O stretching vibration. Also we observe two bands belongs to Al...OH stretching vibration at  $937.04\text{ cm}^{-1}$  and  $916.19\text{ cm}^{-1}$  with higher transmittance percent. the quartz characteristics band from  $694.37\text{ cm}^{-1}$  to  $839.03\text{ cm}^{-1}$  become broader. Finally Al-O-Si, Si-O-Si and Si-O stretching vibration bands from  $426.27\text{ cm}^{-1}$  to  $522.71\text{ cm}^{-1}$  become sharper and triplet bond [9]. Burned initiated Iraqi bentonite FT- IR spectrum (Figure 7. C) Showed the same bands of that in (Figure 7. B) but sharper and with higher transmittance percent, also the band of adsorbed water become a single band at  $3421.7\text{ cm}^{-1}$  mostly due to burning process and the same thing happen with band Al, Mg around water molecule stretching vibration also H...O...H weak bands disappear in this spectrum.

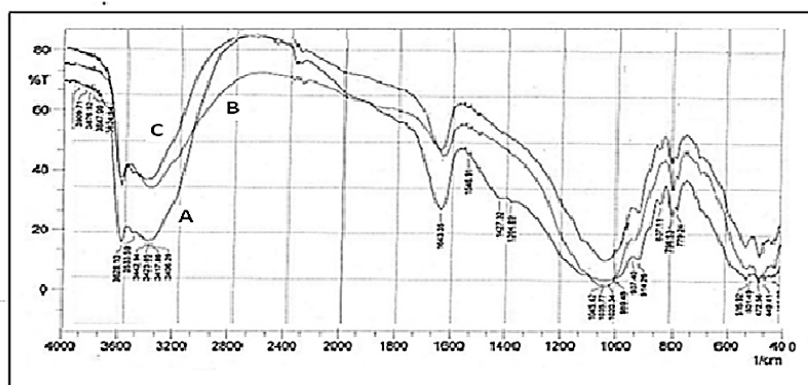


Figure 7. A- FT-IR spectrum for crude Iraqi bentonite (Trifawi), B - FT- IR spectrum for initiated bentonite, C- FT- IR spectrum for burned initiated bentonite

#### 3.2. Calibration graphs.

Three linear calibration curves for ligand (L) were obtained at different pH values (5.5, 7 and 8) (Figs.4,5, and 6), which show that Beer's law was obeyed in the concentration range of (5 – 35)  $\text{mg L}^{-1}$ , Coefficient of determination  $R^2$ , Limit of detection (sensitivity) LOD, in addition to other parameters are given in (Table 3).

Table 3

Spectral characterization and statistical data of the regression equation for Ligand L adsorption on burned Iraqi benronite.

Parameter	Ligand L		
	pH 5.5	pH 7	pH 8
Linearity range (ppm)	5 - 35	5 - 35	5 - 35
Regression equation			
Intercept	0.001271	-0.008714	0.012929
Standard deviation of intercept	0.001506	0.001968	0.000611
slope	0.002889	0.002630	0.001075
Standard deviation of slope	0.000067	0.000088	0.000027
Coefficient of determination R <sup>2</sup>	0.999004	0.997626	0.994927
Standard deviation of the regression	0.000016	0.000027	0.000026
Standard error of Y & X axis STEYX	0.002889	0.002329	0.000723
Limit of detection (sensitivity) LOD	2.046	2.94	2.23
Limit of quantitation LOQ	6.2	8.9	6.7

### 3.3. Effect of adsorbate initial concentration (C<sub>0</sub>) of ligand (L).

The adsorbate concentration on a fixed surface weight of adsorption have been studied by taking 1g clay bed at different PH values (5.5, 7 and 8) using buffer solutions, at room temperature (25±2) °C, plot of (C<sub>0</sub>) values from (Table 2) against removal % of ligand (L), (Figure 8) Elucidate that the highest adsorption of ligand occurs at PH = 7, and with increasing the initial concentration of ligand the amount of ligand removed increased to the extent that we get maximum adsorption capacity of the clay surface.

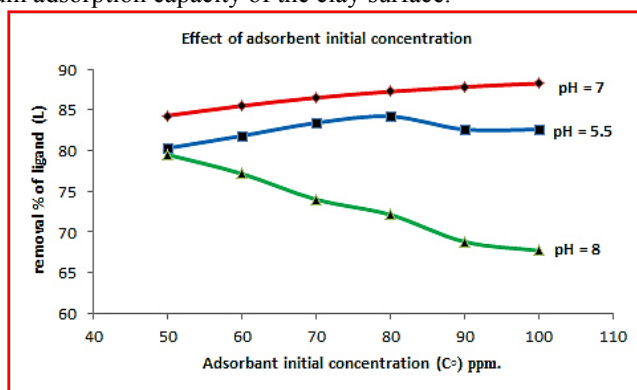


Figure 8. Effect of Adsorbate Initial Concentration of Ligand (L).

### 3.4. Effect of pH.

PH were studied and their impact on the adsorption of ligand (L) On the surface of burned initiated bentonite clay by preparing three ligand (L) solutions of constant concentration (60) ppm adjusted to different pH values (5.5, 7 and 8) using buffer solutions. (10) Mills. of each solution run through three columns of 1g clay bed with constant flow rate (3 drops min<sup>-1</sup>) at room temperature (25±2) °C, then by measuring the absorbance of these solutions through the adsorption column, calculation of removal % of ligand (L) by the clay bed, and plotting removal % against the pH values (Figure 9). It found that the best pH value of adsorption of ligand (L) on clay bed was (pH = 7), and that is due to the neutral character of ligand (L) resulting from the presence of amine groups in the structure of ligand (L).

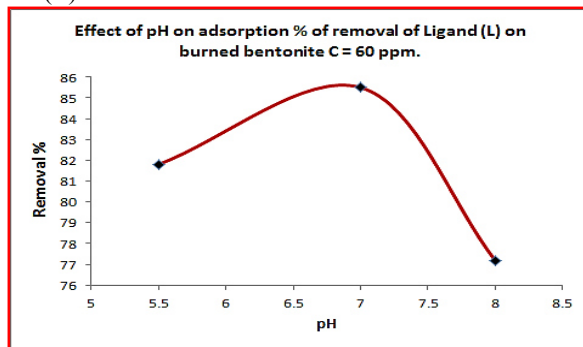


Figure 9. Effect of pH on adsorption % of removal of Ligand (L) on burned bentonite, C = 60 ppm.

### 3.5. Effect of clay weight.

Five different clay weight columns ranged from (1 – 1.8 g) clay bed were prepared for the passage (10 ml) of 90 ppm concentration ligand (L) solution at pH = 7 and to run at constant flow rate of (3 drops/ min.) at room temperature ( $25\pm 2$ ) °C, then by measuring the absorbance of these solutions run through the adsorption column, calculation of removal % of ligand (L) by the clay bed, and plotting removal % against the clay weight (Figure 10) Observed that the highest adsorption of ligand (L) occurs on clay bed of 1.8g weight, this means increasing adsorption with increasing weight of clay to the upper limit of clay capacity, and adsorption surface area.

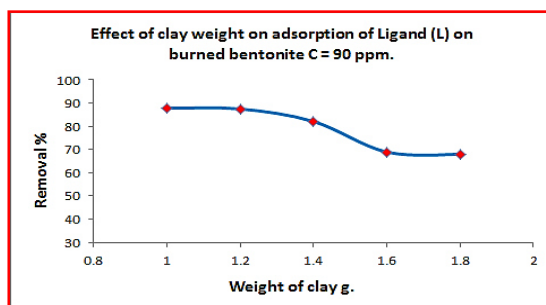


Figure 10. Effect of clay weight on adsorption removal % of Ligand L on burned bentonite, C = 90 ppm.

### 3.6. Effect of ionic strength.

Ionic strength factor was studied by adding different concentrations of sodium chloride (0.1, 0.3, 0.5, and 0.7 M) to four (10 ml) solutions of ligand (L) of constant concentration (90) ppm. Then measuring the absorbance of these solutions run through four adsorption columns of clay bed weight of 1.8 g, calculation of ( $q_e$ ), and plotting ( $q_e$ ) against the molar concentration of NaCl (Figure 11). The graph shows that the adsorption decreases with the increasing of  $\text{Na}^+$  and  $\text{Cl}^-$  ions concentration on the clay bed surface, which is due to high electrostatic interaction of these ions with the clay surface and that hinders ligand (L) adsorption on the clay surface.

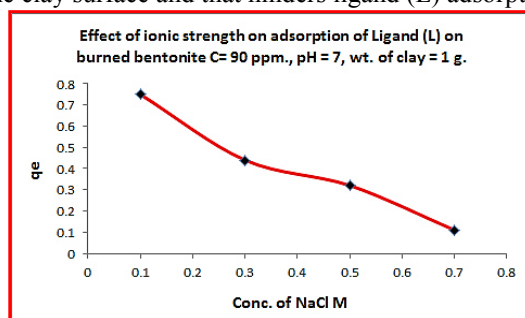


Figure 11. Effect of ionic strength on adsorption of Ligand L on burned bentonite, C = 90 ppm.

### 3.7. Adsorption Isotherms.

Adsorption isotherms are mathematical models that describe the distribution of the adsorbate species among liquid and adsorbent, based on a set of assumptions that are mainly related to the heterogeneity/homogeneity of adsorbents, the type of coverage and possibility of interaction between the adsorbate species. Adsorption data are usually described by adsorption isotherms, such as Langmuir, Freundlich and Temkin isotherms [12]. The set of experimental results as presented in (Figure 12) At room temperature ( $25\pm 2$ ) °C were fitted with the Freundlich, Langmuir and Temkin models. Adsorption isotherms were obtained and the adsorptive capacity interpreted using both models.

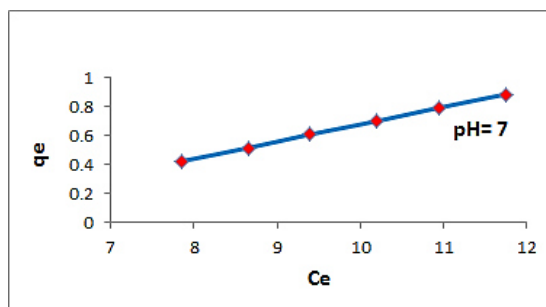


Figure 12. Adsorption isotherm of Ligand L at pH = 7.

#### 3.7.1. The Langmuir isotherm.

The Langmuir model [13, 14] is based on the assumption that the maximum adsorption occurs when a saturated monolayer of solute molecules is present on the adsorbent surface, the energy of adsorption is constant and there

is no migration of adsorbate molecules in the surface plane. The Langmuir isotherm is given by:

$$q_e = \frac{q_m K_L C_e}{1 + K_L C_e} \quad \text{————— (1)}$$

The constants in the Langmuir isotherm can be determined by plotting  $(1/q_e)$  versus  $(1/C_e)$  and making use of above equation rewritten as:

$$\frac{1}{q_e} = \frac{1}{q_m} + \frac{1}{q_m K_L} \frac{1}{C_e} \quad \text{————— (2)}$$

Where  $q_m$  (mg/g) and  $K_L$  (L/mg) are the Langmuir constants, representing the maximum adsorption capacity for the solid phase loading and the energy constant related to the heat of adsorption respectively. The values of  $q_m$  and  $K_L$  can be evaluated from the intercept and the slope of the linear plot of experimental data (Table 4) of  $(1/q_e)$  versus  $(1/C_e)$  (Figure 13) Were found to be 0.70155 mg/g and 0.0483 L/mg, respectively. Also it can be seen from (Figure 13) that the isotherm data fits well the Langmuir equation where the coefficient of determination ( $R^2 = 0.9912$ )

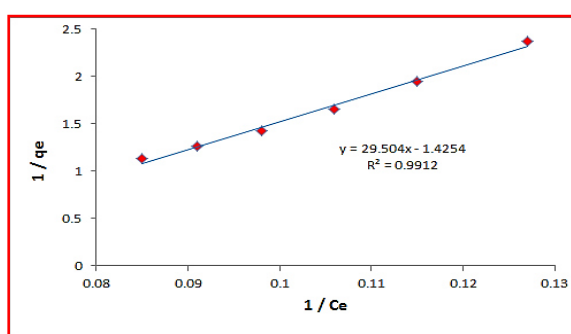


Figure13. Langmuir linear adsorption isotherm of Ligand (L).

Table 4  
 Experimental data of Adsorption Isotherms.

Langmuir		Freundlich		Temkin	
1 / C <sub>e</sub>	1 / q <sub>e</sub>	Log q <sub>e</sub>	Log C <sub>e</sub>	q <sub>e</sub>	Ln C <sub>e</sub>
0.127	2.372	- 0.375	0.894	0.4215	2.060
0.115	1.947	- 0.289	0.937	0.5135	2.157
0.106	1.650	- 0.217	0.973	0.6060	2.240
0.098	1.432	- 0.156	1.008	0.6980	2.322
0.091	1.265	- 0.102	1.039	0.7905	2.393
0.085	1.133	- 0.054	1.070	0.8825	2.463

### 3.7.2. The Freundlich isotherm.

The Freundlich isotherm model [15, 16] is an empirical relationship describing the adsorption of solutes from a liquid to a solid surface and assumes that different sites with several adsorption energies are involved. Freundlich adsorption isotherm is the relationship between the amounts of nickel adsorbed per unit mass of adsorbent,  $q_e$ , and the concentration of ligand at equilibrium,  $C_e$ .

$$q_e = K_f C_e^{1/n} \quad \text{————— (3)}$$

The logarithmic form of the equation becomes,

$$\log q_e = \log K_f + \frac{1}{n} \log C_e \quad \text{————— (4)}$$

Where  $K_f$  and  $n$  are the Freundlich constants, the characteristics of the system.  $K_f$  and  $n$  are the indicators of the adsorption capacity and adsorption intensity, respectively. The ability of Freundlich model to fit the experimental data was examined. For this case, the plot of  $\log C_e$  vs.  $\log q_e$  was employed to generate the intercept value of  $K_f$  and the slope of  $n$ . (Figure 14) The Freundlich constants  $K_f$  and  $n$  were found to be 0.00991 and 0.546 respectively. The Freundlich isotherm is more widely used but provides no information on the monolayer adsorption capacity in contrast to the Langmuir model. Freundlich isotherm fitted well with the coefficient of determination ( $R^2 = 0.9977$ ).

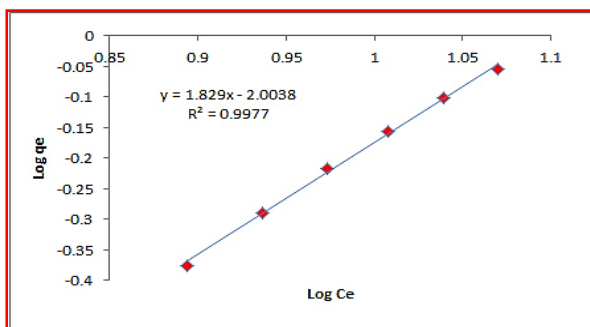


Figure 14. Freundlich linear adsorption isotherm of Ligand (L).

### 3.7.3. The Temkin isotherm.

The Temkin isotherm [17] has been used in the following form:

$$q_e = \frac{RT}{b} \ln(AC_e) \quad \text{-----} \quad (5)$$

A linear form of the Temkin isotherm can be expressed as:

$$q_e = \frac{RT}{b} \ln A + \frac{RT}{b} \ln C_e \quad \text{-----} \quad (6)$$

$$q_e = B \ln A + B \ln C_e \quad \text{-----} \quad (7)$$

Where  $B = \frac{RT}{b}$ , R is gas constant (8.314 J/mol/K), T is Temperature (K)

The sorption data can be analyzed according to Eq. (7). Therefore a plot of  $q_e$  versus  $\ln C_e$  enables us to determine the constants A and B. The values of the Temkin constants A and B are listed in Table 1 and the plot of this isotherm is shown in (Figure 15). The coefficient of determination ( $R^2 = 0.9963$ ) obtained showed that adsorption of ligand (L) also followed Temkin model.

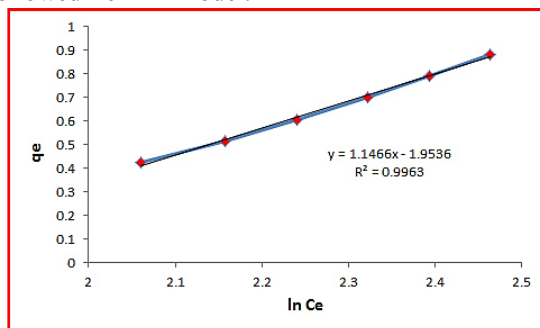


Figure 15. Temkin adsorption isotherm of Ligand (L).

The Langmuir, Freundlich, and Temkin adsorption constants calculated from the corresponding isotherms with the coefficient of determination ( $R^2$ ) are presented in (Table 5).

Table 5.

Isotherm Models Constants and the coefficient of determination ( $R^2$ ) of ligand (L) from Aqueous Solution.

Adsorbent	Langmuir isotherm			Freundlich isotherm			Temkin		
	$q_m$ (mg/g)	$K_L$ (L/mg)	$R^2$	$K_f$	$n$	$R^2$	A (L/g)	B	$R^2$
Initiated burned Iraqi bentonite clay	0.70155	0.0483	0.9912	0.00991	0.5460	0.9977	0.18199	1.1466	0.9963

### 3.8. Effect of flow rate (contact time).

Adsorption of ligand (L) was measured at five different flow rates for a ligand (L) solution of (90) ppm. concentration. From (Figure 16), the plot reveals that the rate of percent ligand (L) removal is higher at low flow rates. This is probably due to higher contact time at these low flow rates. (Table 6) show the calculated parameters that illustrate the importance of flow rate and contact time.



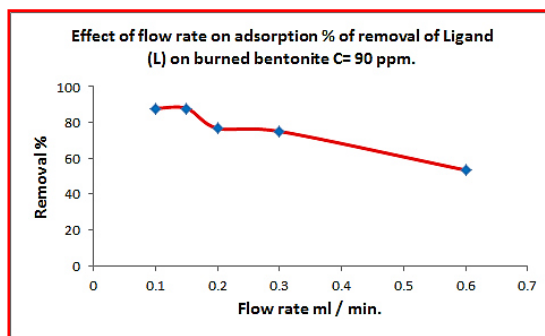


Figure 16. Effect of flow rate on adsorption removal % of Ligand L on burned bentonite, C = 90 ppm.

Table 6

Effect of contact time on the adsorption of (90 mg/mL) Ligand L from aqueous solution.

Initial Conc. (mg/L)	Flow rate drop / min	Flow rate ml / min.	Time min.	Equilibrium Conc. (C <sub>i</sub> ) (mg/L)	Removal %	q <sub>t</sub> (mg/g)	Ln (q <sub>e</sub> -q <sub>t</sub> )	t/q <sub>t</sub>	Equilibrium Time min.
90.000	2	0.1	100.00	10.95	87.83	0.750		133.333	66.666
	3	0.15	66.666	10.95	87.83	0.750		88.888	
	4	0.2	50.000	21.00	76.66	0.690	- 2.8134	72.463	
	6	0.3	33.333	22.50	75.00	0.675	- 2.5902	49.382	
	12	0.6	16.666	42.00	53.33	0.480	- 1.3093	34.721	

### 3.9. Adsorption kinetics.

Kinetic models are used to examine the rate of the adsorption process in the present work; the kinetic data obtained from the studies have been analyzed by using pseudo-first-order and pseudo-second-order models.

The first order equation of Lagergren is generally expressed as follows.

$$dq/dt = k_1(q_e - q_t)$$

where  $q_e$  is the amount of Ligand L adsorbed at equilibrium (mg/g),  $q_t$  is the amount of Ligand L adsorbed at time  $t$  ( $\text{min}^{-1}$ ), and  $k_1$  is the rate constant of pseudo-first-order adsorption. If it supposed that  $q = 0$  at  $t = 0$ , then:

$$\ln(q_e - q_t) = \ln q_e - k_1 t$$

The pseudo-second-order kinetic rate equation is expressed as follows.

$$dq/dt = k_2(q_e - q_t)^2$$

Where  $k_2$  is the rate constant of pseudo-second-order sorption (g/mg/min). The integrated form of Equation when ( $t = 0 \rightarrow t$  and  $q_t = 0 \rightarrow 0q_e$ ) the following expression is obtained:

$$t/q_t = 1/k_2 q_e^2 + t/q_e$$

The rate constant  $k_1$ ,  $k_2$  and  $q_e$  calculated from the slopes and intercepts of the linear plot of  $\ln(q_e - q_t)$  &  $(t/q_t)$  against time respectively (Figures 17, and 18). It is seen that Ligand (L) adsorption is well described by the pseudo second order reaction kinetic. Moreover, the correlation coefficient ( $R^2$ ), of second order reaction kinetic (0.9534) is higher than that of the first order reaction kinetic (0.8585) and greater value of rate constant for the adsorption data.  $q_e$  calculated for the second order reaction kinetic, is higher than the first order reaction kinetic (Table 7).

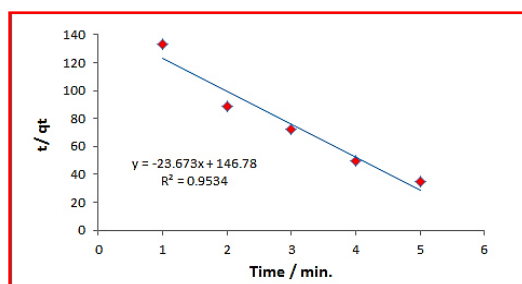


Figure 17. Pseudo-second-order kinetic models for the adsorption of 90 ppm. of Ligand (L) at  $(25 \pm 2)^\circ\text{C}$  under optimum conditions.

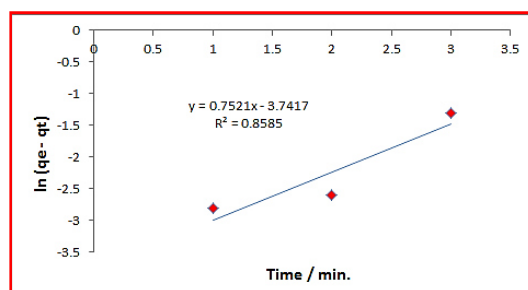


Figure 18. Pseudo-first-order kinetic models for the adsorption of 90 ppm. of Ligand (L) at  $(25\pm 2)^\circ\text{C}$  under optimum conditions.

Table 7

The pseudo- first and second- kinetic order parameters for the adsorption of 90 ppm. of Ligand (L) at  $(25\pm 2)^\circ\text{C}$  under optimum conditions.

qe Experimental (mg/g)	The pseudo-first-order kinetic models			The pseudo-second-order kinetic models		
	qe calculated (mg/g)	K1 (min <sup>-1</sup> )	R2	qe calculated (mg/g)	K2 (g/mg/min)	R2
0.750	0.0237	- 0.7521	0.8585	0.0422	0.00721	0.9534

#### 4. Conclusions

The present investigation elucidate that Iraqi initiated burned bentonite clay mineral is an effective adsorbent for the removal of ligand (L) from aqueous solutions. From the kinetic studies, it is observed that adsorption of ligand (L) is very rapid in the initial stage and decreases while approaching equilibrium. The equilibrium time increases with initial ligand (L) concentration. The percent removal of ligand (L) increases with the increase in adsorbent dosage and decreases with increase in initial ligand (L) concentration. Experimental results are in good agreement with Langmuir, Freundlich and Temkin adsorption isotherm models, and have shown a good fitting to the experimental data. Adsorption of ligand (L) obeys pseudo-second order equation with good correlation.

#### Acknowledgments

We would like to acknowledge Dean of the Faculty of Education Ibn al-Haitham, and the Chemistry department for their financial support. Also thanks for financial support to Dean of the Faculty, and the Chemistry department of College of science, Al- Mustansiriyah University.

#### References

- [1] P.A. Vigato and S. Tamburini, *Coord. Chem. Rev.* 248, 1717 2004.
- [2] C.T.Barboiu, M.Luca, C.Pop, E.Brewster, M.E. Dinculescu. *Eur.J.Med.Chem.*, 31, 597, 1996.
- [3] (a) S.Gaur, *Asian J. chem.* 15 (1) (2003) 250. (b) M.J.Gemi, C.Biles,B.J.Keiser,S.M.Poppe,S.M Swaney, W.G.Tarapley, D.L.Romeso, Y.Yage, *J.Med.Chem.* 43 (5), 1034, 2000.
- [4] E.Ispir,S.Toroglu, A.Kayraldiz, *Transition Met. Chem.* 33, 953, 2008 .
- [5] S.Y. Lee, S.J. Kim, S.Y. Chung and C.H. Jeong, "Sorption of hydrophobic organic compounds onto organo clays", *Journal of Chemosphere (Oxford)*, 55, pp.781-785, 2003.
- [6] Patterson, S.H and Murray, H.H., *Clays*. In: Lefond SI ed. *Industrial minerals and rocks*, 4th - Ed. New York, American Institute of Mining, Metallurgical, and Petroleum Engineers, pp.519– 595, 1983.
- [7] Bentonite, kaolin, and selected clay minerals. (Environmental health criteria ; p.231) , World Health Organization, Geneva, 2005.
- [8] J. H. Potgieter, Adsorption of Methylene Blue on activated carbon: an experiment illustrating both the Langmuir and Freundlich isotherms, *J. Chem.Educ.*68 (4) pp.349- 350, 1991.
- [9] Mohammed H. Abdul Latif, Ali Khalil Mahmood and Maha A. Al –Abayaji, Adsorption of thymol from aqueous solution using granulated surfactant modified Iraqi Na – montmorillonite clay, *Ibn Al-Haitham journal for pure and applied sciences*, vol.(25) no. 1 pp. 266-282, 2012.
- [10] Mahmoud Najim Al-jibouri1, Omar Hamad Shehab AL-Obaidi, Preparation, characterization and theoretical study of metal complexes derived from N5 acyclic ligand, *American Journal of Applied Chemistry*, 2013; 1(3): 37- 42.
- [11] Zlem C. and Demet B. Adsorption of Some Textile Dyes by Hexadecyltrimethylammonium Bentonite, *J. of*

Turk Chem, 25: pp.193-200, 2000.

[12] P. Senthil Kumar R, K. Kirthika, Equilibrium and kinetic study of adsorption of nickel from aqueous solution onto bael tree leaf powder, Journal of Engineering Science and Technology Vol. 4, No. 4, pp. 351 – 363, 2009.

[13] Agyei, N.M.; Strydom, C.A. and Potgieter, J.H.. An investigation of phosphate ion adsorption from aqueous solution by fly ash and slag. Cem. and Concr. Res., 30 (5), pp. 823-826, 2000.

[14] Ho, Y.S. and McKay, G., Competitive sorption of copper and nickel ions from aqueous solution using peat. Adsorption-Journal of the International Adsorption Society, 5(4), pp. 409-417, 1999.

[15] Agyei, N.M.; Strydom, C.A. and Potgieter, J.H., An investigation of phosphate ion adsorption from aqueous solution by fly ash and slag. Cem. and Concr. Res., 30 (5), pp. 823-826, 2000.

[16] Baup, S.; Jaffre, C.; Wolbert, D. and Laplanche, A., Adsorption of pesticides onto granulated activated carbon: determination of surface diffusivities using simple batch experiments. Adsorption, 6 (3), pp. 219-228, 2000.

[17] Wong, K.K.; Lee, C.K.; Low, K.S. and Haron, M.J., Removal of Cu and Pb by tartaric acid modified rice husk from aqueous solutions. Chemosphere, 50(1), pp. 23-28, 2003.